

A Discrete Approach to Feedback Linearization, Yaw Control of an Unmanned Helicopter

Morteza Mohammadzahri^{a,b*}, Arman Khaleghifar^b, Mojtaba Ghodsi^c, Payam Soltani^a, Sami AlSulti^b

^a School of Engineering and the Built Environment, Birmingham City University, UK

^b Mechanical and Industrial Engineering Department, Sultan Qaboos University, Oman

^c School of Energy and Electronic Engineering, University of Portsmouth, UK

Nonlinear control laws often need be implemented with digital hardware. Use of digital control systems leads to communication/processing delays which are widely neglected in control of mechanical systems. This paper proposes a discrete approach to feedback linearization that considers these commonly overlooked delays in design. The proposed approach is shown to both improve the performance and remove the need for continuous derivative terms. In feedback linearization control systems designed in continuous domain, derivative terms are required to speed up the control response of mechanical systems, but disadvantageously cause high sensitivity to noise. The proposed approach was used to design a feedback linearization control system for a common turning manoeuvre of an unmanned helicopter in yaw. At this manoeuvre, the helicopter centroid motion and pitch rotational speed are almost zero. Governing differential equations of the helicopter at this manoeuvre are nonlinear and coupled. A feedback linearization law was proposed to curb nonlinearity and a discrete control system, considering the inevitable delay due to use of digital control systems, was adopted to complete the control law. This innovative approach resulted in less sensitivity to noises and performance boost. Practical limits in terms of control input, rotor speed, sampling frequency and noises of the gyroscope, the tachometer and the acceleration sensor were taken into account in this research. The results show that the proposed control system leads to fast and smooth yaw turns even at a high pitch angle (close to vertical) or in the case of being hit by external objects.

Keywords: Feedback Linearization, Discrete Control Systems, Delay, Noise Sensitivity, Unmanned Helicopters, Yaw Angle

1. Introduction

Unmanned helicopters have been investigated for several decades and are still subject to active research [1-3]. A major component of an unmanned helicopter is its control system, which should provide the helicopter with autonomy. A prominent difficulty in control of unmanned helicopters is their inherited nonlinearity; it is quite well-known that torques of rotors influence the position and angles of the helicopter in a nonlinear way [4-6]. The other issue in control of unmanned helicopters, less renowned than nonlinearity, is time-delays occurring due to use of digital control systems; in reality, the control systems are mostly designed in continuous domain and implemented with digital tools. Hence, the delays induced in digital systems are not taken into account at design stage. The influence of aforementioned time delays in control of helicopters has barely attracted attention of research community [7].

There are three foremost approaches to address nonlinearity of a helicopter in control system design. The first approach is to

use linear controllers based on linearized models, which is common particularly for quadcopters [8-12]. This approach leads to inevitable inaccuracy due to linear approximation. Another popular approach is the use of non-model-based artificial intelligence techniques such as fuzzy logic [13-16] and artificial neural networks [17-19] or a combination of them [20, 21]. This approach removes the need to deal with complex nonlinear mathematical models of helicopters and relies on the collected data and/or experience of human observers/users in the form of linguistic terms [22, 23]. However, this approach demands manned control of the helicopter for some time to obtain required information. The third approach is the use of model-based nonlinear methods. Two popular methods of this approach are sliding mode [24, 25] and feedback linearization [26, 27]. A comparative study shows the superiority of feedback linearization over sliding mode to control an unmanned helicopter when noises are negligible [28]. As a result, feedback linearization was opted, designed and examined in this research. However, feedback linearization has been shown to be less robust against noises, mainly due to derivative terms [28].

*Corresponding Author, Engineering Department, Birmingham City University, Millennium Point, Curzon St, Birmingham B4 7XG, UK

Feedback linearization control systems used in control of unmanned helicopters have continuous linear components with derivative terms [26, 27, 29]. Therefore, if the linear components (and the entire feedback linearization control system) are designed in discrete domain, the issue of sensitivity to noise can be curbed. In addition, in discrete domain, the delays occurring due to digital implementation can be appropriately addressed. As a result, this paper aims to design a feedback linearization control system for a specific manoeuvre of an unmanned helicopter.

An unmanned helicopter has six degrees of freedom, and several modes of operation. As a result, different algorithms have been designed to be employed for landing, take-off or other specific manoeuvres [30-35]. In this research, turning in yaw, or change of yaw angle at fixed pitch and roll angles, is addressed, and a control algorithm dedicated to this task/manoeuvre is designed.

2. Problem Statement and Helicopter Model

This paper focuses on control of an unmanned helicopter driven by electrical motors, when it turns in horizontal plane at a controlled constant pitch, θ , and roll angles, a common and difficult manoeuvre for such machines [36, 37]. It can be reasonably assumed that the centre of helicopter mass nearly does not move in this manoeuvre. With no linear motion, and no change in pitch or roll angle, the helicopter has only one degree of freedom, the yaw angle, ψ , in this specific manoeuvre. Decoupling, presented in [33] has demonstrated that the input voltage to the main rotor has negligible effect on yaw angle; thus, there is a single input for this problem, the input voltage to the rear rotor, U , which affects the rotational speed of the rear rotor, ω , and the yaw angle. Using analysis presented in [4, 19, 27], motion equations during the aforementioned manoeuvre are

$$\begin{cases} \dot{\omega}(t) = \frac{1}{I_R} \left(K_M \frac{U(t) - K_G \omega(t)}{R_R} - \chi_R \operatorname{sgn}(\omega(t)) \omega^2(t) - c_R \omega(t) \right), \\ \ddot{\psi}(t) = \frac{1}{I_V} \left(d \cos \theta(t) \chi_v \operatorname{sgn}(\omega(t)) \omega^2(t) - c_v \dot{\psi}(t) \right), \end{cases} \quad (1)$$

where I_R and I_V stand for moment of inertia for the rear rotor and the whole helicopter, perpendicular to the rear rotor and ground planes, respectively. K , c and χ represent coefficients regarding electrical constants of the rear rotor, mechanical friction and air-related forces. R stands for the rear rotor electrical resistance. d is the projection of distance between mass centre and the rear rotor on the axis perpendicular to the main rotor. Indices M and G clarify the role of rotors in equations, motor (driver) or generator (the source of opposing electromotive force). Complete mathematical model of a helicopter and its reduction to (1) is available in the literature (e.g. in [4, 22]) and is not repeated here. Equations (1) can be re-written as following:

$$\begin{cases} \dot{\omega}(t) = \frac{\overbrace{K_M}^{k_1}}{I_R R} U(t) - \frac{\overbrace{K_M K_G + c_R R}^{k_2}}{R I_R} \omega(t) - \frac{\overbrace{\chi_R}^{k_3}}{I_R} \operatorname{sgn}(\omega(t)) \omega^2(t), \\ \ddot{\psi}(t) = -\frac{\overbrace{c_v}^{k_4}}{I_V} \dot{\psi}(t) + \frac{\overbrace{d \cos \theta \chi_v}^{k_5}}{I_V} \operatorname{sgn}(\omega(t)) \omega^2(t). \end{cases} \quad (2)$$

For a small helicopter with steel body, the following are mechanical and geometrical properties [4]: $K_M=0.03$ N.m/A, $K_G=0.03$ V.s/rad, $I_R=3.2 \times 10^{-7}$ kg.m², $R=0.2$ Ω , $c_R=10^{-5}$ N.m.s/rad, $d=0.1743$ m, $\chi_R=10^{-8}$ N.s²/rad², $I_V=0.032$ kg.m², $c_V=10^{-3}$ N.m.s/rad, $\chi_v=10^{-5}$ N.s²/rad². Therefore, $k_1=4.6875 \times 10^5$, $k_2=1.4094 \times 10^4$ and $k_3=k_4=0.0313$.

Equation (2) will be slightly different, if the control command is generated by a digital control system, with a feedback component and the sample time of t_s . In such a control system, due to the effect of analogue to digital converter clock and other probable communication/processing delays, the measured value is fed into the controller with a delay of t_d . Therefore, the control law generates the control input, U , based on measurements of t_d seconds prior to the current time. This phenomenon exists in all digital closed loop systems; otherwise, an algebraic loop occurs. Therefore, practically, an input-delay is added to (2):

$$\begin{cases} \dot{\omega}(t) = k_1 U(t - t_d) - k_2 \omega(t) - k_3 \operatorname{sgn}(\omega(t)) \omega^2(t), \\ \ddot{\psi}(t) = -k_4 \dot{\psi}(t) + k_5 \operatorname{sgn}(\omega(t)) \omega^2(t). \end{cases} \quad (3)$$

Commonly, due to fast data transmission and process, t_d equals t_s , which is the minimum realisable delay in the system. Only if transmission/process of the sensed data takes longer than the sample time, t_d would be longer than t_s . In such an exceptional case, t_d should be estimated experimentally. This delay seems to be a communication-induced delay rather than an input-induced delay [38]; however, its role in system dynamics, presented in (3), is very similar to an input-induced one. In this paper, for the first time, an approximate discrete approach is proposed to formulate the control problem with partly consideration of the largely neglected delay due to digital implementation, presented in (3).

3. Control Law Development

The following feedback-linearizing control law is proposed for the problem detailed in section 2:

$$U(t) = \frac{k_2}{k_1} \omega(t) + \frac{1}{k_1} \dot{\omega}(t) + \frac{k_3}{k_5 k_1} u_L(t), \quad (4)$$

where u_L is a control command to be found. With incorporating (4) into (3), here is the system dynamics:

$$\begin{aligned} & (\dot{\omega}(t) - \dot{\omega}(t - t_d)) + k_2 (\omega(t) - \omega(t - t_d)) \\ & - \frac{k_3}{k_5} u_L(t - t_d) + \frac{k_3}{k_5} (\ddot{\psi}(t) + k_4 \dot{\psi}(t)) = 0. \end{aligned} \quad (5)$$

3.1. Control Problem Formulation

The system dynamics, presented in (5) was simplified and used to find u_L with two approaches:

i-Conventional Continuous Design Approach: Assuming time delay, t_d , is negligible, (4) and (5) result in the following remaining dynamics:

$$\ddot{\psi}(t) + k_4 \dot{\psi}(t) - u_L(t) = 0. \quad (6)$$

ii-Proposed Approximate Discrete Design Approach: Assuming $\dot{\omega}(t) \approx \dot{\omega}(t-t_d)$ and $\omega(t) \approx \omega(t-t_d)$, (4) and (5) result in the following remaining dynamics:

$$\ddot{\psi}(t) + k_4 \dot{\psi}(t) - u_L(t-t_d) = 0. \quad (7)$$

With the control error $e = \psi_d - \psi$ (8), where ψ_d is the desired yaw angle, assuming that for the regulation problem $\ddot{\psi}_d = \dot{\psi}_d = 0$ (9), error dynamics in continuous and approximate discrete approaches are (10 and 11), respectively:

$$\ddot{e}(t) + k_4 \dot{e}(t) + u_L(t) = 0. \quad (10)$$

$$\ddot{e}(t) + k_4 \dot{e}(t) + u_L(t-t_d) = 0. \quad (11)$$

3-2. Solution of the Control Problem

With approach (i), a classical continuous linear controller was designed for the error dynamics of (10), as detailed in the appendix, to generate u_L .

$$u_L(t) = K_p e(t) + \left(k_4 - 2\sqrt{K_p}\right) \dot{e}(t). \quad (12)$$

Thus, for the regulation problem defined by (8 and 9), the control law of (5) becomes

$$U(t) = \frac{k_2}{k_1} \omega(t) + \frac{1}{k_1} \dot{\omega}(t) + \frac{k_3 K_p}{k_5 k_1} (\psi_d - \psi(t)) + \frac{k_3}{k_5 k_1} \left(2\sqrt{K_p} - k_4\right) \dot{\psi}(t), \quad (13)$$

where K_p is the controller parameter to be chosen.

In the proposed approach (ii), discrete domain was used to find u_L for the system presented in (7), because the delay in (7) leads to nonlinearity in continuous domain. Let us consider an auxiliary variable of u_{LD} :

$$u_{LD}(t) = u_L(t-t_d) \Rightarrow u_{LD}(z) = z^{-\frac{t_d}{t_s}} u_L(z). \quad (14)$$

As a result, (7) can be re-written as

$$\ddot{\psi}(t) + k_4 \dot{\psi}(t) - u_{LD}(t) = 0. \quad (15)$$

Equation (15) can be presented as the following transfer function:

$$\frac{\psi(s)}{u_{LD}(s)} = \frac{1}{s^2 + k_4 s}. \quad (16)$$

Equation (16) was then transferred from s -domain to z -domain using zero-order hold:

$$\frac{\psi(z)}{u_{LD}(z)} = \frac{\frac{t_s k_4 - 1 + e^{-k_4 T}}{k_4^2} z + \frac{1 - t_s k_4 e^{-k_4 T} - e^{-k_4 T}}{k_4^2}}{z^2 - (1 + e^{-k_4 T}) z + e^{-k_4 T}}. \quad (17)$$

Considering (14 and 17):

$$\frac{\psi(z)}{u_L(z)} = z^{-\frac{t_d}{t_s}} \frac{\frac{t_s k_4 - 1 + e^{-k_4 T}}{k_4^2} z + \frac{1 - t_s k_4 e^{-k_4 T} - e^{-k_4 T}}{k_4^2}}{z^2 - (1 + e^{-k_4 T}) z + e^{-k_4 T}}. \quad (18)$$

Due to high speed of processors, it is assumed that control and filtering calculations take a very short time; thus, the minimum delay is enough to avoid an algebraic loop, or $t_d = t_s$ (19). Thus,

$$\begin{aligned} \frac{\psi(z)}{u_L(z)} &= \frac{\overbrace{\frac{t_s k_4 - 1 + e^{-k_4 T}}{k_4^2}}^{b_1} z + \overbrace{\frac{1 - t_s k_4 e^{-k_4 T} - e^{-k_4 T}}{k_4^2}}^{b_2}}{z^3 - \underbrace{(1 + e^{-k_4 T})}_{a_1} z^2 + \underbrace{e^{-k_4 T}}_{a_2} z} \\ &= \frac{b_1 z^{-2} + b_2 z^{-3}}{1 + a_1 z^{-1} + a_2 z^{-2}} = \frac{B(z^{-1})}{A(z^{-1})}. \end{aligned} \quad (20)$$

Considering (8), the following feedback controller may be used to control a system presented by (20):

$$\frac{u_L(z)}{e(z)} = \frac{R(z^{-1})}{S(z^{-1})} = \frac{r_0 + r_1 z^{-1} + \dots + r_{nr} z^{-nr}}{1 + s_1 z^{-1} + \dots + s_{ns} z^{-ns}}. \quad (21)$$

Evidently, the closed-loop transfer function, composed of the feedback controller of (21) and the plant of (20), is

$$G_{CL}(s) = \frac{B(z^{-1})R(z^{-1})}{B(z^{-1})R(z^{-1}) + A(z^{-1})S(z^{-1})}. \quad (22)$$

Considering (20 and 21), in the denominator of (22), the coefficient of the zeroth order of z^{-1} is 1. Thus, the poles of (22) are the values of p_i in (23):

$$\prod_i (1 - z^{-1} p_i) = B(z^{-1})R(z^{-1}) + A(z^{-1})S(z^{-1}) = 0. \quad (23)$$

Any $R(z^{-1})$ and $S(z^{-1})$ which lead to the desirable poles in (23) can be used to form (21).

Equation (23) can be written as (24):

$$B(z^{-1})R(z^{-1}) - A(z^{-1})S(z^{-1}). \quad (24)$$

That is, for any $z = p_i$, the coefficients of each power of z^{-1} should be equal in both sides of (24). Such an equality requires $ns=2$ and $nr=1$ in (21), or

$$R(z^{-1}) = r_0 + r_1 z^{-1}, \quad \text{and} \quad S(z^{-1}) = 1 + s_1 z^{-1} + s_2 z^{-2}. \quad (25)$$

Considering (25), (23) can be re-written as

$$\begin{aligned} \prod_i (1 - z^{-1} p_i) &= \underbrace{(b_1 z^{-2} + b_2 z^{-3})}_{B(z^{-1})} \underbrace{(r_0 + r_1 z^{-1})}_{R(z^{-1})} \\ &+ \underbrace{(1 + a_1 z^{-1} + a_2 z^{-2})}_{A(z^{-1})} \underbrace{(1 + s_1 z^{-1} + s_2 z^{-2})}_{S(z^{-1})} = 0, \end{aligned} \quad (26)$$

$$\text{or} \quad \begin{matrix} 1 \\ z^{-1} \\ z^{-2} \\ z^{-3} \\ z^{-4} \end{matrix} \begin{bmatrix} 1 & 0 & 0 & 0 & 0 \\ a_1 & 1 & 0 & 0 & 0 \\ a_2 & a_1 & 1 & b_1 & 0 \\ 0 & a_2 & a_1 & b_2 & b_1 \\ 0 & 0 & a_2 & 0 & b_2 \end{bmatrix} \begin{bmatrix} 1 \\ s_1 \\ s_2 \\ r_0 \\ r_1 \end{bmatrix} = \Gamma, \quad (27)$$

where Γ is a column consisting of coefficients of different orders of z^{-1} in $\prod_i (1 - z^{-1} p_i)$.

\mathbf{X} in (27) or the column of coefficients of controller (21) can be found with (28), if \mathbf{T} is non-singular,

$$\mathbf{X} = \mathbf{T}^{-1} \Gamma. \quad (28)$$

Considering (21, 25 and 28) and Z transform of derivative, the control law of (4) can be presented as (29) in the proposed discrete approach:

$$U(t) = \left(\frac{k_2}{k_1} + \frac{1-z^{-1}}{k_1 t_s} \right) \omega(t) + \frac{k_3}{k_5 k_1} \frac{r_0 + r_1 z^{-1}}{1 + s_1 z^{-1} + s_2 z^{-2}} (\psi_d - \psi(t)). \quad (29)$$

4. Implementation of Control Laws

Implementation of the control laws of continuous and proposed discrete approaches, Eqs. (13 and 29), requires definition of K_p and desired poles, p_i s, of Eq.(23), respectively. These final steps of design were completed considering practical limits to assure realistic simulations and conclusions. If these practical limits were not considered, we would have apparently excellent performance in simulation, which could not be realized. Here is the list of parameters or variables in which practical limits were considered for them:

1. Sampling time/frequency: The electrical part of the system is very fast. If nonlinearities were disregarded in (3), the time constant of the system would be $k_4^{-1} < 7.1 \times 10^{-5}$ s. As a result, a sampling time, at least, comparable with this value should be opted. In this research, the sampling time/frequency of 10^{-4} s/ 10 kHz was chosen. A higher sampling frequency could lead to better performance particularly with undermining the ignored delays of (5); however, too high sampling frequency (rate) imposes excessive expense for hardware.

2. Rear rotor rotational speed or ω : Although, use of feedback linearization removes ω from linear control system design in subsections 3-1 and 3-2; however, this value cannot be unbounded, and a realistic limit of [-1000 1000] rad/s was considered for it.

3. Control input or U in (4): The essence of control input is voltage and should be supplied with a DC voltage supply; a limit of [-24 24]V was assumed for U to be realistic. In order to investigate system's behaviour beyond U saturation limits, the transfer function of (16) was employed; the input to the transfer function is u_{LD} , in the proposed approach. Let us assume both ω and U are saturated. Based on (29), u_L/ u_{LD} will have a fixed value of A immediately or after t_S seconds. Then,

$$\text{Eq.(16)} \Rightarrow \psi(s) = \frac{1}{s^2 + k_4 s} u_{LD}(s) \xrightarrow{\text{saturation}} \psi(s) = \frac{1}{s^2 + k_4 s} \frac{A}{s} = -\frac{A}{k_4^2 s} + \frac{A}{k_4 s^2} + \frac{A}{k_4^2 (s + k_4)} \Rightarrow$$

$$\psi(t) = -\frac{A}{k_4^2} + \underbrace{\frac{A}{k_4}}_{\text{critical term}} t + \frac{A}{k_4^2} e^{-k_4 t}. \quad (30)$$

Equation (30) demonstrates that the control system is unstable when saturated; thus, saturation limits should be considered in design. A similar reasoning can be offered for the continuous approach, where u_L replaces u_{LD} in (30).

Design of (13 and 26) was completed based on aforementioned triple limits.

4.1. Implementation of Control Law Derived from Continuous Approach

Figure 1 shows the response of (13) in turning the helicopter 20° in yaw with different values of K_p , while the pitch angle is maintained around 30° . Overshoots are evident; although, the design, presented in the appendix, aimed to prevent them for any value of K_p . This is influenced by non-cancelled nonlinearities (including saturations) and the delays neglected to form (6). Maximum overshoot and the settling time seem to be reversely related to each other. Disadvantageously, the control law of (13) adds some repeating overshoot to the system anyway.

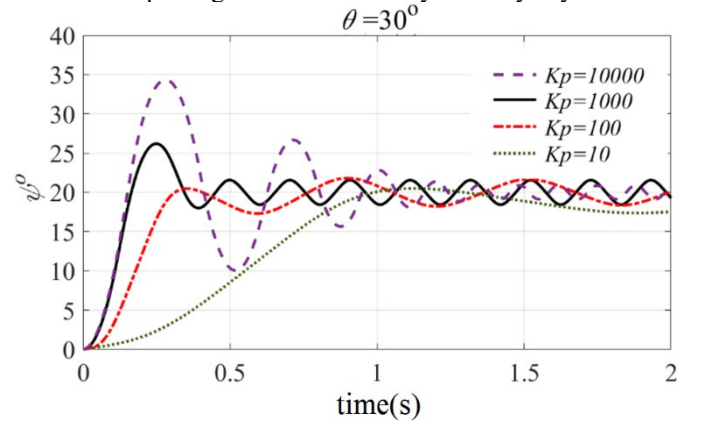


Fig. 1. The response of (13) (continuous approach) with different values of K_p

4.2. Implementation of Control Law Derived from the Proposed Discrete Approach

In order to finalise the design of (29) control law, derived out of the proposed discrete approach, the desired poles of the closed loop system, p_i s of (23), should be chosen. Any discrete pole with an absolute value below 1 is stable, and closed loop poles closer to 0 result in faster convergence [39]. However, a fast converging pole pushes the control input towards saturation limits very quickly, and the system will face the risk of instability as presented in (30). Appendix B presents the result for some too fast poles and demonstrate the effect of saturation. A single desired discrete pole of 0.999 can lead to a stable and still very fast closed loop system. With a sampling frequency of 10 kHz, such a discrete pole equals a continuous pole of -10.005.

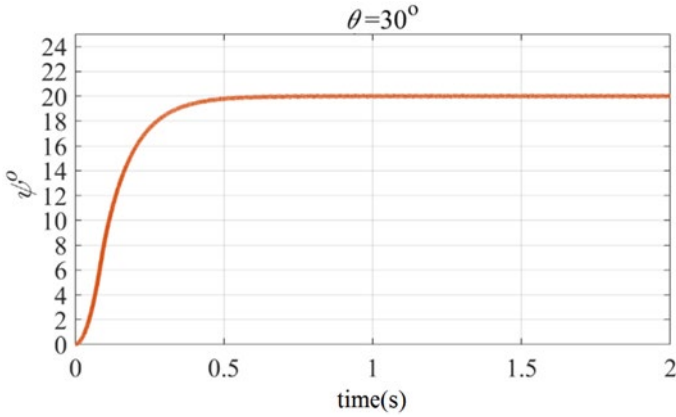


Fig. 2. The response of (36) (derived out of the proposed discrete approach), where the closed loop system of (23) has a single discrete pole of 0.999

Having a single real pole removes the chance for overshoot, if nonlinearities are ignorable. Figure 2 confirms this expectation.

With this single pole of $p_l=0.999$, the following Γ was used in (27):

$$\Gamma = \begin{bmatrix} 1 \\ -0.999 \\ 0 \\ 0 \\ 0 \end{bmatrix}. \quad (31)$$

Hence, with use of (28), the linear controller of (21) becomes

$$\frac{u_L(z)}{e(z)} = \frac{R(z^{-1})}{S(z^{-1})} = \frac{1.0025 \times 10^8 - 1.0015 \times 10^8 z^{-1}}{1 + 1.001z^{-1} + 0.5008z^{-2}}. \quad (32)$$

Considering the values in section 2, the control law of Eq. (29) can be written as Eq. (33):

$$U(t) = (0.0514 - 0.0213z^{-1})\omega(t) + \frac{1.4168 \times 10^{-5} + 1.4154 \times 10^{-5} z^{-1}}{1 + 1.001z^{-1} + 0.5008z^{-2}}(\psi_d - \psi(t)). \quad (33)$$

5. Results and Discussion

Comparison of Figs. 1 and 2 demonstrate the superiority of the proposed discrete approach to control system design. Therefore, in this section, test results of the proposed control law of (33) is only presented with the following initial values: $\psi(0)=\omega(0)=0$ and $\dot{\psi}(0)=0.1\text{rad/s}$.

The control system deals with three sensors of the unmanned model helicopter: a gyroscope to measure yaw angle rate, $\dot{\psi}$ (to be used in (33)) [40], a piezoresistive angular acceleration sensor [41] and a tachometer [42] to measure the rear rotor angle and its rate, ω and $\dot{\omega}$. Yaw angle, ψ , is calculated through integration of its rate. Gyroscope, angular acceleration sensor and the tachometer have random noises in the range of $\pm 5\%$, $\pm 0.1\%$ and $\pm 3\%$ of their measured values. Several

simulations demonstrated that sensor noises have a negligible influence on the performance of control law of (33), so that, the curves of simulations with and without noise are hardly recognisable. Same noises can seriously affect the performance of a control system including an error derivative, as demonstrated in [43].

Figure 3 demonstrates two test results, both with the $\psi_d=40^\circ$, but at the pitch angles of 30° and 80° . The latter, close to a vertical situation, witnesses an overshoot of over 13° . This manoeuvre requires higher input voltage and rear rotor rotational speed and pushes the operating area towards saturation.

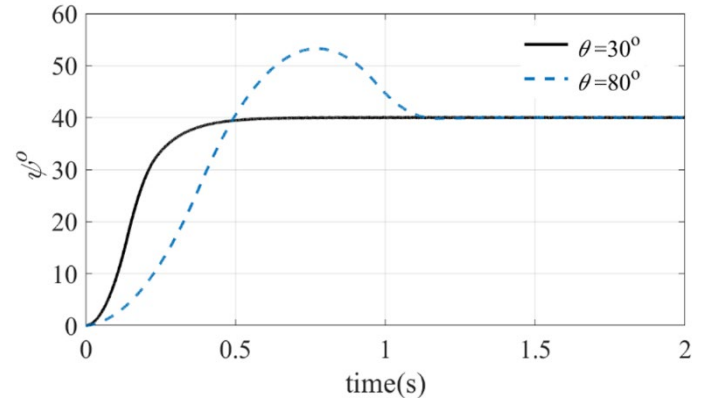


Fig. 3. The performance of the control law of Eq. (33) at different pitch angles with the same desired yaw angle of 40°

It is probable that an unmanned aerial vehicle hits an object during flight. Such an occurrences was simulated with sudden exertion an external torque, T , for a limited time. During torque exertion, yaw dynamics (below equation of (1)) is

$$\ddot{\psi}(t) = \frac{1}{I_V} (d \cos \theta(t) \chi_v \text{sgn}(\omega(t)) \omega^2(t) - c_v \dot{\psi}(t) + T). \quad (34)$$

Figure 4 depicts the response of the control system with desired yaw angles of 10° , 30° and 50° , where the unmanned helicopter is hit in/against the direction of its rotation for 0.001s at time $t=1$ s with 50 and 100 N.m external torques. Considering Euler's law, these values of external torque are severe and can apply extreme angular acceleration of 1562.5 and 3125 rad/s^2 on the helicopter body. This figure shows that the control system of Eq. (33) can return the unmanned helicopter to the desired conditions very fast. Expectedly, at the pitch angle of 80° , close to the vertical situation, damping the disturbance is more difficult.

Eq.(34) can also simulate the situation where pitch or roll angles deviate their references. Such a situation leads to non-zero pitch or roll rotational speeds. As an instance, the presence of pitch rotation causes a torque, T_θ , in yaw plane [4, 19, 27], shown in Eq.(35), which can replace T in (34).

$$T_\theta = -I_M \omega_M \omega_\theta \sin \theta. \quad (35)$$

where $I_M=4.7\times 10^{-7}$ kg.m² and ω_M are the moment of inertia and the rotational speed of the main rotor, respectively. Even with extremely high value of 1000 rad/s for both rotational speeds in (35), the absolute value of T_θ would be less than 0.5 N.m.

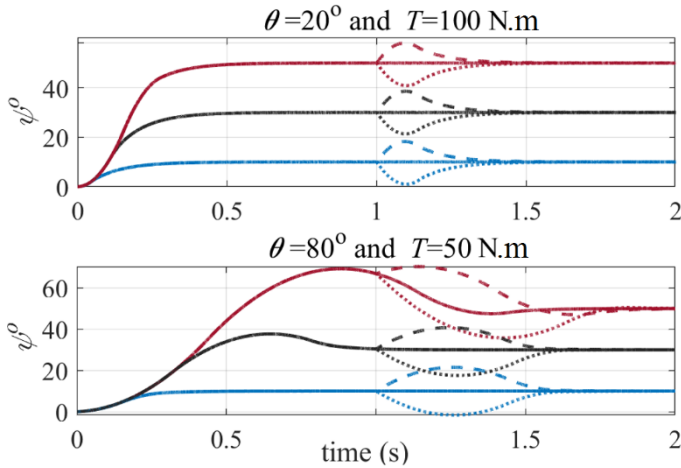


Fig. 4. The response the unmanned helicopter with the control law of (33) to disturbance at different pitch angles and desired yaw angles

If the models and the control laws presented in this paper are compared to the ones in the literature, two innovations can be highlighted:

- (i) Considering the inherent delay of digital control systems, e.g. in (5 and 7)
- (ii) Design of feedback linearization control system for unmanned helicopters in discrete domain to take the delay into account, (29 and 33)

Figures 1-4 show the aptness of the proposed design approach.

This research also underlines two advantages of control systems with discrete linear controllers over the ones with continuous linear controllers:

- 1) In discrete domain, delays can be embedded into linear discrete models without adding nonlinearity; while, delays are nonlinear (exponential) components in continuous domain.
- 2) Discrete controllers tend to be less sensitive to noises compared to continuous controllers with derivatives.

The first advantage lets a more accurate model, i.e. (7), be used in control system design, a reason for higher performance. Equation (7) would be a nonlinear equation in Laplace domain. A Smith-predictor-based control system or a similar method might be able to use (7) in continuous domain; however, that would impose an extra loop and its complexities to the control system [44]. The second afore-listed advantage removes a well-known drawback of feedback linearization control of unmanned helicopters: high sensitivity to noises [28]. Classical continuous controllers, widely used within feedback linearization control systems of helicopters and other mechanical system, often include derivatives as discussed in the appendix. These derivatives, which are non-existent in discrete controllers, are a major source of sensitivity to noises.

As to Problem Statement, the proposed control system and results are for the prevalent manoeuvre presented in section 2. For more complex manoeuvres, e.g. when the centre of mass witnesses a significant motion while yawing, the mathematical model and consequently the control law would be different. However, the demonstrated advantages of the proposed design approach in discrete domain, including (i) performance improvement as a result of considering inherent data transfer/processing delays, and (ii) reduction of sensitivity to noises, due to removal of derivative terms plausibly remain valid.

6. Conclusion

This paper deals with the control of an unmanned helicopter in yaw turning, while the pitch and roll angles are well regulated, a frequent manoeuvre. Nonlinear and coupled governing differential equations of the manoeuvre dynamics compel the use of a nonlinear method; hence, feedback linearization was opted. Use of feedback linearization to control unmanned helicopters has been reported in the literature; however, (a) a delay existing in all digital closed loop systems has been disregarded, and (b) discrete domain design methods (which can deal with the aforementioned delay) have not been employed. Both of these were considered/used in this research resulting in high performance as well as robustness against noises and disturbances (external hits).

A feedback linearization control system with a linear continuous component for the unmanned helicopter was designed, reported in the appendix, to be compared to the proposed control system; it was shown that a derivative term is essential for such a control system to have a reasonably fast response. However, derivatives are very sensitive to noises, and this is why low robustness against noises is a known weak point of helicopter control systems based on feedback linearization. Use of discrete domain design removed this drawback and resulted in an excellent robustness against noises.

In addition, it was mathematically proven that a control input, voltage to the rear rotor, beyond its saturation limit leads to instability. As a result, in discrete control system design, a closed loop pole rather close to stability border was chosen to moderate convergence speed and shorten the time that the control limit lies beyond its saturation limits.

7. References

- [1] G. Cai, B. M. Chen, and T. H. Lee, *Unmanned rotorcraft systems* (Springer Science & Business Media, 2011).
- [2] A. Mohiuddin, T. Tarek, Y. Zweiri, and D. Gan, *A survey of single and multi-UAV aerial manipulation*, *Unmanned Systems*,8(02)(2020) 119-147.
- [3] H. Virani, D. Liu, and D. Vincenzi, *The Effects of Rewards on Autonomous Unmanned Aerial Vehicle (UAV) Operations Using Reinforcement Learning*, *Unmanned Systems*, 9(04)(2021) 349-360.
- [4] K. Unneland, "Application of model predictive control to a helicopter model," Norwegian University of Science and Technology, 2003.

- [5] M. Mohammadzaheri and L. Chen, Hybrid intelligent control of a lab model helicopter pitch dynamics, in *International Conference on Intelligent and Advanced Systems*, (Kuala Lumpur, Malaysia, 2007), pp. 162-166.
- [6] W. Chang, J. H. Moon, and H. J. Lee, *Fuzzy Model-Based Output-Tracking Control for 2 Degree-of-Freedom Helicopter*, Journal of Electrical Engineering & Technology, **12**(4)(2017) 1649-1656.
- [7] Y. Chen, X. Yang, and X. Zheng, *Adaptive neural control of a 3-DOF helicopter with unknown time delay*, Neurocomputing, **307**(2018) 98-105.
- [8] Z. Jiang, J. Han, Y. Wang, and Q. Song, Enhanced LQR control for unmanned helicopter in hover, in *1st International Symposium on Systems and Control in Aerospace and Astronautics*, (Harbin, China, 2006), pp. 1437-1443.
- [9] K. Pan, Y. Chen, Z. Wang, H. Wu, and L. Cheng, Quadrotor Control based on Self-Tuning LQR, in *37th Chinese Control Conference* (Wuhan, China, 2018), pp. 9974-9979.
- [10] C. Liu, J. Pan, and Y. Chang, PID and LQR trajectory tracking control for an unmanned quadrotor helicopter: Experimental studies, in *35th Chinese Control Conference* (Chengdu, China, 2016), pp. 10845-10850.
- [11] J. van den Berg, "Extended LQR: Locally-optimal feedback control for systems with non-linear dynamics and non-quadratic cost," in *Robotics Research*, 1st ed: Springer, 2016, pp. 39-56.
- [12] M. Ghodsi, T. Ueno, and T. Higuchi, *Improvement of magnetic circuit in levitation system using HTS and soft magnetic material*, IEEE Transactions on Magnetics, **41**(10)(2005) 4003-4005.
- [13] M. J. Fotuhi and Z. Bingul, Position and Trajectory Fuzzy Control of a Laboratory 2 DOF Double Dual Twin Rotor Aerodynamical System, in *27th IEEE International Symposium on Industrial Electronics* (Cairns, Australia, 2018), pp. 277-282.
- [14] M. Mohammadzaheri and A. Mirsepahi, *Design of an anti-overshoot Mamdani-type fuzzy-adaptive controller for yaw angle control of a model helicopter*, International Journal of Intelligent Systems Technologies and Applications, **4**(3-4)(2008) 386-398.
- [15] M. Mohammadzaheri and L. Chen, Anti-overshoot control of model helicopter's yaw angle with combination of fuzzy controller and fuzzy brake, in *International Conference on Intelligent and Advanced Systems*, (Kuala Lumpur, Malaysia, 2007), pp. 99-103.
- [16] M. Ghodsi, N. Hosseinzadeh, A. Özer, H. R. Dizaj, Y. Hojjat, N. G. Varzeghani, *et al.*, *Development of Gasoline Direct Injector using giant magnetostrictive materials*, IEEE Transactions on Industry Applications, **53**(1)(2017) 521-529.
- [17] A. Razzaghian and R. K. Moghaddam, Robust Adaptive Neural Network Control of Miniature Unmanned Helicopter, in *Iranian Conference on Electrical Engineering* (Mashad, Iran, 2018), pp. 801-805.
- [18] M. Shirzadeh, H. J. Asl, A. Amirkhani, and A. A. Jalali, *Vision-based control of a quadrotor utilizing artificial neural networks for tracking of moving targets*, Engineering Applications of Artificial Intelligence, **58**(2017) 34-48.
- [19] M. Mohammad-Zaheri and L. Chen, Design of an Intelligent Controller for a Model Helicopter Using Neuro-Predictive Method with Fuzzy Compensation, in *World Congress on Engineering*, (London, UK, 2007).
- [20] M. Mohammadzaheri and L. Chen, *Hybrid Neuro-Predictive-Fuzzy Algorithm for a Model Helicopter's Yaw Angle Control*, Engineering Letters, **16**(1)(2008) 18-26.
- [21] A. C. Aras and O. Kaynak, Trajectory tracking of a 2-dof helicopter system using neuro-fuzzy system with parameterized conjunctors, in *IEEE/ASME International Conference on Advanced Intelligent Mechatronics*, (Besacon, France, 2014), pp. 322-326.
- [22] M. Mohammadzaheri and L. Chen, *Intelligent predictive control of a model helicopter's yaw angle*, Asian Journal of Control, **12**(6)(2010) 667-679.
- [23] M. Mohammadzaheri and L. Chen, *Design and stability discussion of an hybrid intelligent controller for an unordinary system*, Asian Journal of Control, **11**(5)(2009) 476-488.
- [24] Z. Jia, J. Yu, Y. Mei, Y. Chen, Y. Shen, and X. Ai, *Integral backstepping sliding mode control for quadrotor helicopter under external uncertain disturbances*, Aerospace Science and Technology, **68**(2017) 299-307.
- [25] H. Sira-Ramirez, M. Zribi, and S. Ahmad, *Dynamical sliding mode control approach for vertical flight regulation in helicopters*, IEE Proceedings-Control Theory and Applications, **141**(1)(1994) 19-24.
- [26] C.-W. Lin, T.-H. S. Li, and C.-C. Chen, *Feedback linearization and feedforward neural network control with application to twin rotor mechanism*, Transactions of the Institute of Measurement and Control, **40**(2)(2018) 351-362.
- [27] M. Lopez-Martinez, J. Diaz, M. Ortega, and F. Rubio, Control of a laboratory helicopter using switched 2-step feedback linearization, in *American Control Conference* (Boston, USA, 2004), pp. 4330-4335.
- [28] D. Lee, H. J. Kim, and S. Sastry, *Feedback linearization vs. adaptive sliding mode control for a quadrotor helicopter*, International Journal of control, Automation and systems, **7**(3)(2009) 419-428.
- [29] A. Mokhtari, N. K. M'Sirdi, K. Meghriche, and A. Belaidi, *Feedback linearization and linear observer for a quadrotor unmanned aerial vehicle*, Advanced Robotics, **20**(1)(2006) 71-91.
- [30] B. Geranmehr, E. Khanmirza, and S. Kazemi, *Trajectory control of aggressive maneuver by agile autonomous helicopter*, Proceedings of the Institution of Mechanical Engineers, Part G: Journal of Aerospace Engineering, **233**(4)(2019) 1526-1536.
- [31] H. Huang, G. M. Hoffmann, S. L. Waslander, and C. J. Tomlin, Aerodynamics and control of autonomous quadrotor helicopters in aggressive maneuvering, in *IEEE International Conference on Robotics and Automation* (Kobe, Japan, 2009), pp. 3277-3282.
- [32] T. Merz, S. Duranti, and G. Conte, "Autonomous landing of an unmanned helicopter based on vision and inertial sensing," in *Experimental Robotics*, 9th ed: Springer, 2006, pp. 343-352.

- [33] A. Yamane, "Unmanned helicopter, takeoff method of unmanned helicopter, and landing method of unmanned helicopter," ed: Google Patents, 2007.
- [34] Q. Zheng, Z. Xu, H. Zhang, and Z. Zhu, *A turboshaft engine NMPC scheme for helicopter autorotation recovery maneuver*, *Aerospace Science and Technology*, **76**(2018) 421-432.
- [35] C. Luo, W. Zhao, Z. Du, and L. Yu, *A neural network based landing method for an unmanned aerial vehicle with soft landing gears*, *Applied Sciences*, **9**(15)(2019) 2976.
- [36] L. Ding, R. Ma, H. Wu, C. Feng, and Q. Li, *Yaw control of an unmanned aerial vehicle helicopter using linear active disturbance rejection control*, *Proceedings of the Institution of Mechanical Engineers, Part I: Journal of Systems and Control Engineering*, **231**(6)(2017) 427-435.
- [37] T.-Q. Le, Y.-C. Lai, and C.-L. Yeh, *Adaptive tracking control based on neural approximation for the yaw motion of a small-scale unmanned helicopter*, *International Journal of Advanced Robotic Systems*, **16**(1)(2019) 1-9.
- [38] M. Wu, Y. He, and J.-H. She, *Stability analysis and robust control of time-delay systems* (Springer, 2010).
- [39] I. D. Landau and G. Zito, *Digital Control Systems* (Springer London, 2006).
- [40] V. Passaro, A. Cuccovillo, L. Vaiani, M. De Carlo, and C. E. Campanella, *Gyroscope technology and applications: A review in the industrial perspective*, *Sensors*, **17**(10)(2017) 1-22.
- [41] S. J. Ovaska and S. Valiviita, *Angular acceleration measurement: A review*, in *IEEE Instrumentation and Measurement Technology Conference*, (St. Paul, USA, 1998), pp. 875-880.
- [42] Shimpo, "Digital Tachometers/Counters," Nidec, Ed., ed. Kyoto, Japan, 2014.
- [43] M. Mohammadzahi, H. Ziaiefar, M. Ghodsi, and I. B. Bahadur, *Yaw control of an unmanned helicopter with feedback linearization*, in *1st International Conference on Unmanned Vehicle Systems-Oman (UVS)*, 2019), pp. 1-5.
- [44] M. Mohammadzaheri and R. Tafreshi, *An Enhanced Smith Predictor Based Control System Using Feedback-feedforward Structure for Time-delay Processes*, *The Journal of Engineering Research [TJER]*, **14**(2)(2017) 156-165.

Appendix A. Linear Control System Design

This appendix reports the design of a linear controller based on system/error dynamics presented in (6)/(10).

A.1. Proportional Controller

With $u_L = Ke$, Eq. (10) becomes a homogenous differential equation of

$$\ddot{e}(t) + k_4 \dot{e}(t) + Ke(t) = 0. \quad (\text{A.1})$$

with the following characteristic equation and time response:

$$\begin{cases} s^2 + k_4 s + K = 0, \\ e(t) = K_{e1} e^{p_1 t} + K_{e2} e^{p_2 t}. \end{cases} \quad (\text{A.2})$$

Then, the poles of error dynamics, p_1 and p_2 , are

$$p_{1,2} = \frac{-k_4 \pm (k_4^2 - 4K)^{0.5}}{2}. \quad (\text{A.3})$$

A negative K always leads to a positive pole and instability; hence, K should be positive. For positive K and k_4 , the real part of the poles is always negative; thus, the system is stable with the dominant pole of (A.4):

$$p_d = \frac{-k_4 + (k_4^2 - 4K)^{0.5}}{2}. \quad (\text{A.4})$$

Since k_4 is positive, the greatest absolute value of the dominant pole, leading to the fastest convergence of the error towards zero, happens at $k_4^2 - 4K = 0$. (A.5)

Moreover, in order to have real poles (to assure non-oscillating response), it is required that $k_4^2 - 4K \geq 0$. (A.6)

As a result, the fastest non-oscillating convergence of the control error towards zero happens when (A.5) is met or

$$K = \frac{k_4^2}{4}. \quad (\text{A.7})$$

This value of K leads to twin poles of $-0.5 k_4$; that is, the time constant of the response is $2\pi/\text{pole}$ or $4\pi/k_4$. Therefore, with the values provided in section 2 for the parameters of a steel unmanned helicopter, the time constant of the response is 402 s. This response is obviously too slow. Hence, proportional controller is not a good choice to generate u_L .

A.2. Proportional Derivative Controller

An alternative to improve classical linear controllers with slow responses is to add derivatives. Thus, a proportional-derivative (PD) linear control law of

$$u_L(t) = K_p e(t) + K_d \dot{e}(t). \quad (\text{A.8})$$

was opted. With combination of (10 and A-8), error dynamics will be

$$\ddot{e}(t) + (k_4 + K_d) \dot{e}(t) + K_p e(t) = 0, \quad (\text{A.9})$$

with characteristic equation of $s^2 + (k_4 + K_d)s + K_p = 0$. (A.10) Thus, the closed loop poles are

$$p_{1,2} = \frac{-(k_4 + K_d) \pm ((k_4 + K_d)^2 - 4K_p)^{0.5}}{2}. \quad (\text{A.11})$$

With similar reasons to the ones provided for (A.1-3), (46) is the requirement to have the fastest non-oscillating convergence of the error towards zero:

$$\begin{cases} (k_4 + K_d)^2 - 4K_p = 0, \\ \text{or } K_d = 2\sqrt{K_p} - k_4. \end{cases} \quad (\text{A.12})$$

Thus, resultant twin non-oscillating poles are:

$$p_{1,2} = \frac{-(k_4 + K_d)}{2}. \quad (\text{A.13})$$

As a result, time constant is $4\pi/(k_4 + K_d)$, which can be quite short for a high positive K_d . As to (A.12), (A.8) can be presented as (12).

Appendix B. Too Fast Poles and Saturation

As mentioned in section 4, e.g. in Eq.(30), while the control command is saturated, the system is unstable. As mentioned in subsection 4.2, the pole of 0.999 was chosen to avoid too high values of control command and saturation. Figure 5 shows the system undesirable behaviour, if the control system is designed based on too fast poles, i.e. discrete poles too close to zero.

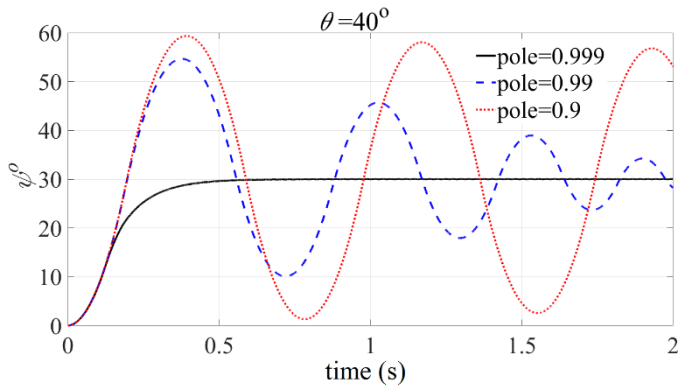


Fig. 5. The response of (29) with the parameters derived so that the closed loop system of (23) has a single discrete pole of 0.9, 0.99 and 0.999.